

¹H NMR based sulfonation reaction kinetics of wine relevant thiols in comparison with known carbonyls

Sofia Tachtalidou^a, Apostolos Spyros^b, Nicolas Sok^a, Silke S. Heinzmann^c, Franck Denat^d, Philippe Schmitt-Kopplin^{c,e}, Régis D. Gougeon^a, Maria Nikolantonaki^{a,*}

^a Université Bourgogne Franche-Comté, Institut Agro, Université Bourgogne, INRAE, UMR PAM 1517, Institut Universitaire de la Vigne et du Vin – Jules Guyot, 21000 Dijon, France

^b NMR Laboratory, Department of Chemistry, University of Crete, P.O. Box 2208, Voutes Campus, 71003 Heraklion, Crete, Greece

^c Research Unit Analytical BioGeoChemistry, Helmholtz Munich, Ingolstädter Landstraße 1, 85764, Neuherberg, Germany

^d Institut de Chimie Moléculaire de l'Université de Bourgogne, UMR 6302, CNRS, Université Bourgogne Franche-Comté, 21078 Dijon, France

^e Analytical Food Chemistry, Technical University Munich, TUM, Maximus-von-Imhof-Forum 2, 85354 Freising, Germany

ARTICLE INFO

Keywords:

Oxidation
Chardonnay
Sulfur dioxide
Glutathione
Acetaldehyde

ABSTRACT

Sulfite addition is a common tool for ensuring wines' oxidative stability via the activity of its free and weakly bound molecular fraction. As a nucleophile, bisulfite forms covalent adducts with wine's most relevant electrophiles, such as carbonyls, polyphenols, and thiols. The equilibrium in these reactions is often represented as dissociation rather than formation. Recent studies from our laboratory demonstrate, first, the acetaldehyde sulfonate dissociation, and second, the chemical stability of cysteine and epicatechin sulfonates under wine aging conditions. Thus, the objective of this study was to monitor by ¹H NMR the binding specificity of known carbonyl-derived SO₂ binders (acetaldehyde and pyruvic acid) in the presence of S-containing compounds (cysteine and glutathione). We report that during simulated wine aging, the sulfur dioxide that is rapidly bound to carbonyl compounds will be released and will bind to cysteine and glutathione, demonstrating the long-term sulfur dioxide binding potential of S-containing compounds. These results are meant to serve as a complement to existing literature reviews focused on molecular markers related to wines' oxidative stability and emphasize once more the importance of S-containing compounds in wine aging chemical mechanisms.

1. Introduction

The year 1487 marked a turning point in the history of winemaking. In that year, a Prussian royal decree officially permitted the use of the wine additive sulfur dioxide (or SO₂) for the first time. To help preserve their wines during transport, Dutch and English wine traders regularly burned sulfur candles inside barrels before filling them. To this day, sulfites remain common preservatives used for antimicrobial and/or antioxidant (browning) stability in fruits, vegetables and processed foods (Friedman, 1996). Sulfur dioxide is commonly added as bisulfite (HSO₃⁻) rather than its gaseous form and has been used for many purposes in wine production. Firstly, it is an efficient antiseptic that provides protection against detrimental microorganisms, particularly bacteria (Bartowsky, 2009). SO₂ also has high antioxidant activity as it inhibits or delays the deteriorating effects of oxidation (Wissemann & Lee, 1980). Up to 30 mg/L of SO₂ can be frequently produced in the must

as a natural product derived from yeast metabolism according to OIV (Stockley et al., 2021).

Sulfur dioxide is present in wine in free and bound forms. The free and weakly bound SO₂ are the active forms that provide antioxidant protection to the wine. At wine pH (between 3 and 4), HSO₃⁻ is the predominant form, representing about 94–99% of the total free form, the rest being molecular SO₂, since SO₃²⁻ is usually negligible (Aberl & Coelhan, 2013; Goncalves et al., 2010). Bisulfite is a nucleophile and forms covalent adducts with electrophiles, such as carbonyls, ketoacids, sugars, quinones, indoles, anthocyanins and other compounds, forming sulfonated adducts (Arapitsas et al., 2018; Waterhouse et al., 2016). The equilibrium in these reactions is often represented as dissociation rather than formation. The dissociation constant (K_d) has been calculated mainly for carbonyl compounds (Burroughs & Sparks, 1973), phenolic compounds and sugars (Waterhouse et al., 2016) summarized in our recent publication (Tachtalidou et al., 2024). Based on the same study,

* Corresponding author at: Université de Bourgogne, UMR PAM, 2 rue Claude Ladrey, 21000 Dijon, France.

E-mail address: maria.nikolantonaki@u-bourgogne.fr (M. Nikolantonaki).

<https://doi.org/10.1016/j.foodchem.2024.138944>

Received 13 October 2023; Received in revised form 12 February 2024; Accepted 2 March 2024

Available online 5 March 2024

0308-8146/© 2024 The Authors. Published by Elsevier Ltd. This is an open access article under the CC BY license (<http://creativecommons.org/licenses/by/4.0/>).

we have described the chemical mechanism of sulfonation of both free sulfur containing compounds (-SH) and flavan-3-ols under wine aging conditions (presence/absence of oxygen and Fe (II)). Under wine oxidation conditions, regardless dissolved oxygen and Fe (II) concentrations, thiols and flavan-3-ols form sulfones that are stable over time. Additionally, the quantitative data in young and aged bottled wines showed increasing concentrations in aged wines. This highlights the contribution of the as yet unexplored role of thiols and polyphenols on the stable bound fraction of SO₂ and proves the necessity of reconsidering the strength of the SO₂-binders when they are in competition.

Moreover, in recently published studies, non-targeted mass spectrometry-based metabolomic analyses provided evidence that white wine's antioxidant metabolome is essentially composed of sulfur containing compounds, principally peptides (36% CHONS and 20% CHOS) and amino acids (Karbowski et al., 2019; Nikolantonaki et al., 2018; Romanet et al., 2021; Roullier-Gall et al., 2019). The addition of sulfites during the pre-fermentative steps of winemaking impacts the chemical diversity of amino acids, carbohydrates and phenolics (Roullier-Gall et al., 2017), while indole and polyphenol sulfonated products were reported as molecular markers related to aged wines (Arapitsas et al., 2014; Arapitsas et al., 2018). Recently, Nikolantonaki et al. (2022) after combining FTICR-MS based metabolomics and sensory analysis of a vertical series of white wines, evidenced that in their majority S- containing molecular features possessing between 4 and 12 O atoms appeared to be related to stable aged wines indicating the importance of sulfonation reaction instead of dimerization reactions on wines' oxidative stability during aging. In the same study, molecular networking suggested that sulfonation of peptides, aldehydes and polyphenols could be a fundamental reaction related to white wines' oxidative stability.

In order to gain control over the wine oxidation mechanisms, it is clear that a solid fundamental understanding of SO₂ reactivity with key wine relevant compounds is needed, as SO₂ is an important additive in winemaking. Deciphering its reactivity with other wine components is crucial for the fine-tuning of SO₂ addition with respect to what is actually needed for a given wine. Thus, the next step to unravel the complicated mechanisms involved in sulfonation reactions of thiols would be the monitoring of the competition between thiols and carbonyls for the available SO₂ during aging. In the present study, 1D and 2D NMR spectroscopy was used for the identification and characterization of targeted carbonyls (acetaldehyde and pyruvic acid) and thiols (cysteine and glutathione) sulfonation products under wine acidic conditions. ¹H NMR was further used to profile the competitive kinetics of carbonyl and thiol sulfonation reactions in controlled (low and high) oxygenation levels and molecular ratios in order to simulate barrel and bottle aging conditions.

2. Materials and methods

2.1. Chemicals

Ultrapure water (18.2 MΩ) was obtained from Millipore (Germany). Acetaldehyde, pyruvic acid, glutathione, L-cysteine, ethanol (>99.8% MS grade), tartaric acid and trimethylsilylpropionic acid sodium salt (TSP) were purchased from Sigma-Aldrich (St. Louis, MO, USA). Sodium hydroxide was purchased from ChemLab and D₂O from Euriso-top (Saarbrücken, Germany). Sodium metabisulfite (Na₂S₂O₅) was purchased from Merck (Darmstadt, Germany) and dissolved directly in model wine solutions to obtain the desired SO₂ concentrations (referred to as commercial SO₂). Ethanol (MS grade > 99.8%) and formic acid were purchased from Sigma-Aldrich (St. Louis, MO, USA). Sodium formate was purchased from Sigma Aldrich, while methanol (MS grade) and acetonitrile (MS grade) were purchased from Biosolve Chimie (Dieuze, France).

2.2. Synthesis of cysteine and glutathione sulfonates for NMR characterization (exp.1)

Glutathione or cysteine (70 mM each) was dissolved into a sodium bisulfite model wine solution (12% v/v ethanol, 5 g/L tartaric acid, pH 3.5 adjusted by drops of NaOH at room temperature) in a 1/5 M ratio and stirred for 5 min at room temperature. The sample preparation occurred under aerobic conditions and the reaction was monitored for 6 weeks by ¹H NMR spectroscopy.

2.3. Kinetic study of commercial sulfur dioxide reaction with carbonyls and thiols in mixture (exp.2)

In a model wine solution (12% v/v ethanol, 5 g/L tartaric acid, pH 3.5) with SO₂ (Na₂S₂O₅), 10 mM of each of the following compounds, acetaldehyde, pyruvic acid, cysteine and glutathione, were mixed in 3 different binder/SO₂ molar ratios in order to simulate the enological conditions related to barrel aging (1/4), bottle aging at one year (1/1) and late bottle aging (2/1). Thus, the concentrations of HSO₃⁻ in the three ratios were 160 mM, 40 mM and 20 mM respectively. During the sample preparation for the first two conditions, the model wine solutions were purged with air, while the third one (late bottle aging) was prepared under anaerobic conditions in the presence of nitrogen flow (bubbling). All 20 mL amber vials were full without any headspace and were immediately sealed. Reactions took place in duplicate at room temperature (298 K).

2.4. LC-QToF-MS characterization of reaction products (for exp.1)

For LC-QToF-MS analyses, the synthesized sulfonated adducts in model wine (5 μL) were injected onto an Acquity BEH C18 column (1.7 μm, 100 × 2.1 mm, Waters, Guyancourt, France). A standard reverse-phase linear gradient with acidified water with 5% of acetonitrile (0.1% v/v of formic acid) and acidified acetonitrile (0.1% v/v of formic acid) was run over 15 min at a flow rate of 400 μL/min, and the eluent was monitored for negative ions by a MaXis plus MQ ESI-Q-TOF mass spectrometer (Bruker, Bremen, Germany). Source parameters were 2 bar nebulizer pressure, 10 L/min dry gas flow at 200 °C, 4500 V capillary voltage and 500 V end plate off set. Before batch analysis, the mass spectrometer was calibrated using sodium formate in enhanced quadrupole mode. The mass range was between 100 and 600 *m/z* in negative and positive ionization mode. Quality controls were analyzed before and throughout each batch, to verify the stability of the LC-MS system. All samples were analyzed randomly. The instrument control and the analysis of the data were performed by the "Data Analysis" software.

2.5. Acquisition of NMR spectra and apparatus

For exp.1, NMR analyses were performed on a Bruker 500 MHz spectrometer at constant temperature 298 K. Samples were mixed with 100 μL of D₂O that contained 0.1% of TSP. TSP was used as an internal standard for quantification. ¹H NMR spectra were obtained by using WET multiple solvent suppression experiment for simultaneous suppression of water and ethanol proton peaks. 2D NMR spectra were performed for the identification of free and bound cysteine and glutathione. The 2D acquisition parameters for the COSY experiment were as follows: The standard cosygpprqf Bruker pulse sequence was used, with a spectral width of 6009.615 Hz (F2) and 6001.588 Hz (F1), the acquisition time was 0.17 s, 48 scans and 16 dummy scans. Acquisition parameters for the ¹H – ¹³C HSQC experiment were as follows: The hsqcedetgpsisp2.3 Bruker pulse sequence, which also incorporates DEPT editing of the signals based on carbon multiplicity (methine, methylene, methyl) was used, with a spectral width of 6009.615 Hz in the F2 dimension and 25,153.443 Hz in the F1 dimension. The acquisition time was 0.17 s, 64 scans and 16 dummy scans. Acquisition parameters for

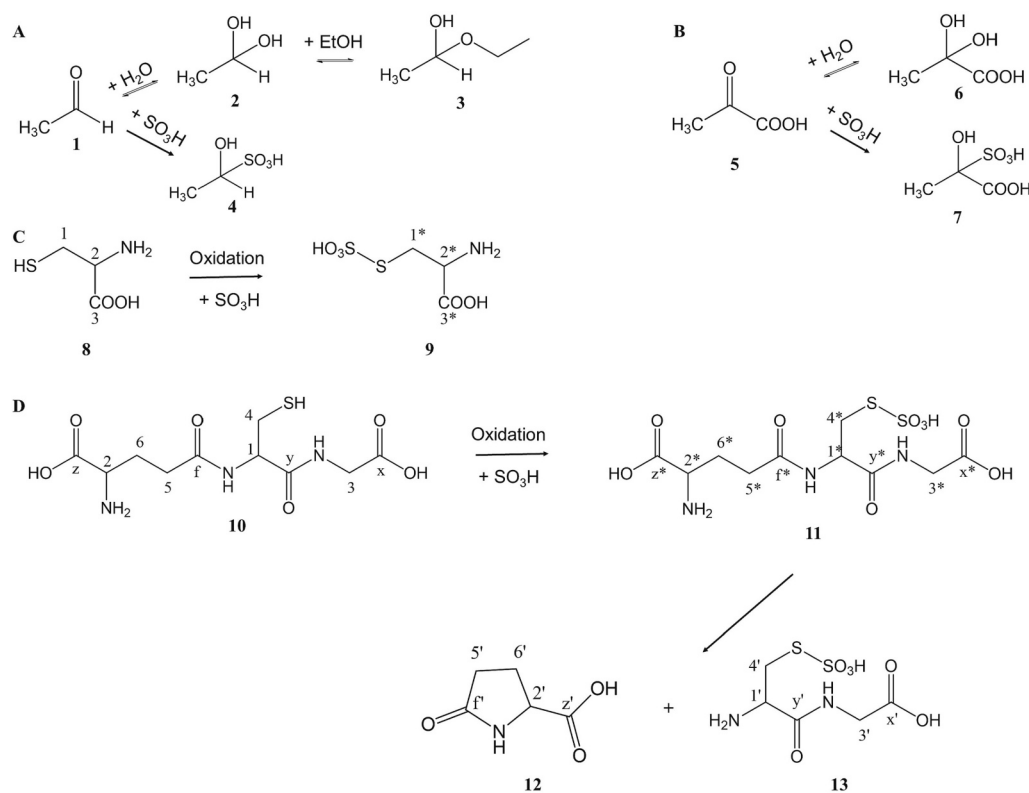


Fig. 1. Structures of identified free and sulfonated acetaldehyde (A); pyruvic acid (B); cysteine (C) and glutathione (D) derived compounds in model wine (12% v/v ethanol, 5 g/L tartaric acid, pH 3.5) at room temperature. Acetaldehyde (1), hydrated acetaldehyde (2), acetaldehyde ethyl hemiacetal (3), acetaldehyde sulfonate (4), pyruvic acid (5), hydrated pyruvic acid (6), pyruvic sulfonate (7), cysteine (8), cysteine sulfonate (9), glutathione (10), glutathione sulfonate (11), pyroglutamic acid (12), cysteinylglycine sulfonate (13).

the $^1\text{H} - ^{13}\text{C}$ HMBC experiment were as follows: The hmbcgp1pdqf Bruker pulse sequence was used, with a spectral width 6493.506 Hz in the F2 dimension and 30,196.844 Hz in the F1 dimension. Acquisition time was 0.15 s, and 72 scans with 16 dummy scans were acquired. All NMR data were processed using Topspin 3.5 NMR (Bruker) software.

For exp.2, NMR analysis was performed on a Bruker 600 MHz spectrometer using a cryoprobe at 298 K. Samples were mixed with 100 μL of D_2O that contained 0.1% of TSP. ^1H NMR spectra were obtained by using WET multiple solvent suppression experiment for simultaneous suppression of water and ethanol proton peaks. Acquisition time was 2.72 s, number of scans 32 and dummy scans 16. All NMR data were processed using Topspin 4.0.6 NMR (Bruker) software.

2.6. NMR and MS description of studied compounds

NMR and MS assignments of acetaldehyde and pyruvic sulfonates were based on published data. (Nikolantonaki et al., 2015) Assignments of free and sulfur bound cysteine and glutathione as well as the reaction products identified in the mixture, pyroglutamic acid and cysteinylglycine sulfonate, are reported as follows:

Cysteine (8): ^1H NMR (500 MHz, $\text{H}_2\text{O} + \text{D}_2\text{O}$) δ 3.02 (1H, dd), 3.10 (1H, dd), 3.97 (1H, dd). ^{13}C NMR (125 MHz, $\text{H}_2\text{O} + \text{D}_2\text{O}$) δ 27.79 (C1), 58.88 (C2), 173.07 (C3). ESI-MS (m/z) $[\text{M} - \text{H}]^+$, calc. For $\text{C}_3\text{H}_7\text{O}_2\text{SN}$ 122.0270; measured, 122.0268; retention time: 0.63 min.

Cysteine sulfonate (9): ^1H NMR (500 MHz, $\text{H}_2\text{O} + \text{D}_2\text{O}$) δ 3.49 (1H, H1a*, dd), 3.66 (1H, H1b*, dd), 4.18 (1H, H2*, dd). ^{13}C NMR (125 MHz, $\text{H}_2\text{O} + \text{D}_2\text{O}$) δ 35.54 (C1*), 55.05 (C2*), 172.42 (C3*). ESI-MS (m/z) $[\text{M} - \text{H}]^-$, calc. For $\text{C}_3\text{H}_7\text{O}_5\text{S}_2\text{N}$, 199.9692; measured, 199.9706; retention time: 0.67 min.

Glutathione (10): ^1H NMR (500 MHz, $\text{H}_2\text{O} + \text{D}_2\text{O}$) δ 2.16 (2H, H6*, m), 2.55 (2H, H5*, m), 2.94 (2H, H4*, dd), 3.80 (1H, H2*, m), 3.94 (2H, H3*, dd), 4.50 (1H, H1*, dd). ^{13}C NMR (125 MHz, $\text{H}_2\text{O} + \text{D}_2\text{O}$) δ 29.06

(C6*), 34.05 (C5*), 28.32 (C4*), 57.17 (C2*), 46.35 (C3*), 58.55 (C1*), 179.10 (Cx*), 174.51 (Cy*), 177.72 (Cf*), 176.83 (Cz*). ESI-MS (m/z) $[\text{M} - \text{H}]^-$, calc. For $\text{C}_{10}\text{H}_{17}\text{O}_6\text{S}_2\text{N}_3$, 306.0765; measured, 306.0765; retention time: 0.74 min.

Glutathione sulfonate (11): ^1H NMR (500 MHz, $\text{H}_2\text{O} + \text{D}_2\text{O}$) δ 2.18 (2H, H6*, m), 2.54 (2H, H5*, m), 3.40 (1H, H4a*, dd), 3.56 (1H, H4b*, dd), 3.84 (1H, H2*, m), 3.95 (2H, H3*, dd), 4.80 (1H, H1*, dd). ^{13}C NMR (125 MHz, $\text{H}_2\text{O} + \text{D}_2\text{O}$) δ 26.64 (C6*), 31.81 (C5*), 36.17 (C4*), 54.44 (C2*), 42.48 (C3*), 53.75 (C1*), 174.34 (Cx*), 172.66 (Cy*), 174.98 (Cf*), 174.08 (Cz*). ESI-MS (m/z) $[\text{M} - \text{H}]^-$, calc. For $\text{C}_{10}\text{H}_{17}\text{O}_9\text{S}_2\text{N}_3$, 386.0333; measured, 386.0331; retention time: 0.65 min.

Pyroglutamic acid (12): ^1H NMR (500 MHz, $\text{H}_2\text{O} + \text{D}_2\text{O}$) δ 2.14 (1H, H6a', m), 2.54 (1H, H6b', m), 2.41 (2H, H5', m), 4.30 (1H, H2', m). ^{13}C NMR (125 MHz, $\text{H}_2\text{O} + \text{D}_2\text{O}$) δ 25.98 (C6'), 30.05 (C5'), 57.57 (C2'), 182.04 (Cf'), 169.14 (Cz'). ESI-MS (m/z) $[\text{M} - \text{H}]^-$, calc. For $\text{C}_5\text{H}_7\text{O}_3\text{N}$, 128.0353; measured, 128.0350; retention time, 0.75 min.

Cysteinylglycine sulfonate (13): ^1H NMR (500 MHz, $\text{H}_2\text{O} + \text{D}_2\text{O}$) δ 3.55 (1H, H4a', dd), 3.65 (1H, H4b', dd), 3.95 (2H, H3', dd), 4.50 (1H, H1', dd). ^{13}C NMR (125 MHz, $\text{H}_2\text{O} + \text{D}_2\text{O}$) δ 35.88 (C4'), 42.48 (C3'), 53.13 (C1'), 172.33 (Cx'), 168.41 (Cy'). ESI-MS (m/z) $[\text{M} - \text{H}]^-$, calc. for $\text{C}_5\text{H}_{10}\text{O}_6\text{S}_2\text{N}_2$, 256.9907; measured, 256.9921; retention time: 0.68 min.

3. Results and discussion

3.1. Identification and quantification of thiol sulfonation reaction products in comparison with known carbonyl sulfonates

1D and 2D NMR spectroscopy were used for the identification and quantification of free and bound forms of tested compounds, as proposed by Nikolantonaki et al. (2015). NMR spectroscopy allows the direct online monitoring of sulfonation reactions equilibria without dilution or artifacts related to any pH modifications. Two carbonyl compounds

Table 1

NMR assignments of identified free and sulfonated acetaldehyde; pyruvic acid; cysteine and glutathione derived compounds in model wine (12% v/v ethanol, 5 g/L tartaric acid, pH 3.5) at room temperature. The peaks used for the quantification of the sulfonated adducts are presented in *italics*.

Compound	¹ H (ppm)	¹³ C (ppm)	Assignment
Acetaldehyde (1)	9.66	207.2 [†]	-CHO
	2.23	30.8 [†]	-CH ₃
Acetaldehyde hydrated (2)	5.23	88.8 [†]	-CH
	1.35	23.8 [†]	-CH ₃
Acetaldehyde Ethyl Hemiacetal (3)	4.94	94.69 [†]	-CH
	3.77	63.3 [†]	-CH ₂ (Ha)
	3.51	63.3 [†]	-CH ₂ (Hb)
	1.17	14.87 [†]	-CH ₃
	1.30	22.6 [†]	-CH ₃
Acetaldehyde sulfonate (4)	4.54	81.0 [†]	-CH
	1.46	17.6 [†]	-CH ₃
	2.44	26.6 [†]	-CH ₃
Pyruvic acid (5)	2.44	26.6 [†]	-CH ₃
Pyruvic acid hydrated (6)	1.57	25.8 [†]	-CH ₃
Pyruvic sulfonate (7)	1.67	21.3	-CH ₃
Cysteine (8)	3.02	27.8 [‡]	-CH ₂ (H1a)
	3.10	27.8 [‡]	-CH ₂ (H1b)
	3.97	56.4 [‡]	-CH (H2)
Cysteine sulfonate (9)	-	173.1 [‡]	-COOH (C3)
	3.49	35.5	-CH ₂ (H1a*)
	3.66	35.5	-CH ₂ (H1b*)
	4.18	54.9	-CH (H2*)
	-	172.4	-COOH (3*)
Glutathione (10)	2.16	29.1	-CH ₂ (H6)
	2.55	34.1	-CH ₂ (H5)
	2.94	28.3	-CH ₂ (H4)
	3.80	57.2	-CH (H2)
	3.94	46.4	-CH ₂ (H3)
	4.50	58.6	-CH (H1)
	-	179.1	-COOH (Cx)
	-	174.5	-CO (Cy)
	-	177.7	-CO (Cf)
	-	176.8	-COOH (z)
Glutathione sulfonate (11)	2.18	26.6	-CH ₂ (H6*)
	2.54	31.8	-CH ₂ (H5*)
	3.40	36.2	-CH ₂ (H4*a)
	3.56	36.2	-CH ₂ (H4*b)
	3.84	54.4	-CH (H2*)
	3.95	42.5	-CH ₂ (H3*)
	4.80	53.8	-CH (H1*)
	-	174.3	-COOH (Cx*)
	-	172.7	-CO (Cy*)
Pyroglutamic acid (12)	-	175.0	-CO (Cf*)
	-	174.1	-COOH (Cz)
	4.30	57.57	-CH (H2)
	2.41	30.1	-CH ₂ (H5)
	2.14 / 2.54	26.0	-CH ₂ (H6)
Cysteinylglycine sulfonate (13)	-	182.0	-CO (Cf)
	-	169.1	-COOH (Cz)
	4.50	53.1	-CH (H1)
	3.95	42.5	-CH ₂ (H3)
	3.55 / 3.65	35.9	-CH ₂ (H4)
-	172.3	-COOH (Cx)	
-	168.4	-CO (Cy)	

[†] (Nikolantonaki et al., 2015).

[‡] <https://hmdb.ca/metabolites/HMDB0000574>

(acetaldehyde and pyruvic acid) and two sulfur containing compounds (cysteine and glutathione) were tested separately in model wine solution for their binding potential at different molecular ratios of available SO₂ and oxygen. Glutathione and cysteine sulfonates gave a yield of 82% and 36%, respectively, at 6 weeks. In accordance with literature, the yields of acetaldehyde and pyruvic acid sulfonates were 100% after a few minutes when SO₂ was in excess (Deshmukh et al., 2009). The chemical structures of the identified compounds and their assignments are presented in Fig. 1 and Table 1, respectively. 2D NMR spectra used for the assignment of cysteine and glutathione sulfonates are presented in Supplementary Information (Figs. S1-S8). In the case of glutathione sulfonate 2D COSY, HSQC and HMBC experiments revealed the presence of

additional peaks attributed to pyroglutamic acid and cysteinylglycine sulfonate (Supplementary Information Fig. S5). This indicates that the scission of glutathione sulfonate can occur under wine acidic conditions at room temperature in a few weeks. It should be noted that the mechanism of the non-enzymatic self-degradation of glutathione has been already reported at a pH range 6.2–7.4 (Zecchini et al., 2019). In that respect, cysteinylglycine sulfonate can be considered as a by-product of glutathione sulfonate and explain its fate during wine aging.

Fig. 2 shows the ¹H NMR spectrum and the quantification assignments of all tested free and bound compounds in the mixture of model wine at room temperature after one month of reaction (binder/SO₂: 1/4). When SO₂ is added in the model wine solution in the presence of carbonyls and thiols, it is expected that acetaldehyde ($K_d = 1.5 \times 10^{-6}$) and pyruvic acid ($K_d = 1.55 \times 10^{-4}$) will be the first compounds to bind with it. After the addition of SO₂, the doublet of the -CH₃ (2.23 ppm) group of free acetaldehyde is protected and shifted to a higher field region at 1.46 ppm. In the same way, when pyruvic acid is dissolved in model wine, the hydrated form is initially produced (6). After the addition of SO₂, the singlet of the -CH₃ (2.44 ppm) group of pyruvic acid is also protected and shifted to a higher field region at 1.67 ppm. On the other hand, the sulfonation reactions of thiols are slow and incomplete, thus both free and bound forms of cysteine and glutathione are present during the first weeks of reaction. Free cysteine contributes two doublet of doublets (dd) peaks at 3.02 and 3.10 ppm originating from the protons of the CH₂ group and a dd at 3.97 ppm from the methine proton. Its sulfonated adduct appears with two doublets of the doublets, one at 3.49 and the other at 4.18 ppm. In fact, 2D NMR (Figs. S1-S4 Supplementary Information) experiments showed that the -CH₂ group of cysteine sulfonate forms two different dd peaks because the magnetic environment of each proton is different. Thus, the chemical shift for one proton of the -CH₂ group appears at 3.49 ppm and the other at 3.66 ppm. More specifically, in COSY 2D NMR experiment (Fig. S2), a correlation crosspeak between a proton (dd) at 3.49 ppm and a proton at 3.66 ppm is observed (this proton is not visible in the 1D proton spectrum as it is hidden under the ethanol peak). Also, these two protons are correlated to a dd at 4.18 ppm, leading to the conclusion that H1a and H1b can be assigned to the two protons of the CH₂ group of cysteine sulfonate, while H2 is assigned to the proton of the CH group of the same compound. In the HSQC spectrum (Fig. S3) we observe a correlation peak between proton H1a* at 3.49 ppm and its attached carbon C1, at 35.55 ppm, a spectral region characteristic of carbons that are chemically bound to sulfur. Additionally, it is observed that proton H2* at 4.18 ppm is correlated with a carbon at 55.01 ppm, a spectral region characteristic of C–N carbons bound to a nitrogen. So, we conclude that cysteine sulfonation takes place at the -SH side and not at the -NH₂ unit. The HMBC spectrum (Fig. S4) showed that all these three protons (H1a*, H1b* and H2*) have a long-range H–C correlation with the carboxyl carbon C3, verifying that sulfonation does not occur at the -COOH group. This characterization is consistent with the known literature (Zecchini et al., 2019).

Glutathione is a tripeptide composed of glutamate, cysteine and glycine. The identification of glutathione sulfonate was achieved by 2D NMR experiments (Figs. S6-S8). In the COSY spectrum (Fig. S6) the correlation between the protons H5*-H6*, H2*-H6*, 2 H4* and H4*-H1* is observed. The HSQC spectrum (Fig. S7) also presented the correlation between a proton and its carbon, but to confirm the recommended structure, HMBC 2D experiment was necessary (Fig. S8). In HMBC, the correlation between proton H3* and the carboxyl carbon (Cx*), proton H2* and the carbonyl carbon (Cz*) and proton H5* and the carbonyl carbon (Cf*) are observed. Thus, we can clearly confirm the chemical structure of glutathione sulfonate, which similar to cysteine, results from the reaction with sulfites at the sulfhydryl group, forming an S–S bond.

In Fig. S5 (Supplementary Information), there are additional peaks (marked with apostrophes as H and C in Figs. S5-S8) coming from pyroglutamic acid and cysteinylglycine sulfonate, compounds that are produced from the dissociation of glutathione sulfonate. In the COSY spectrum (Fig. S6), we observed the correlation between the two H4*

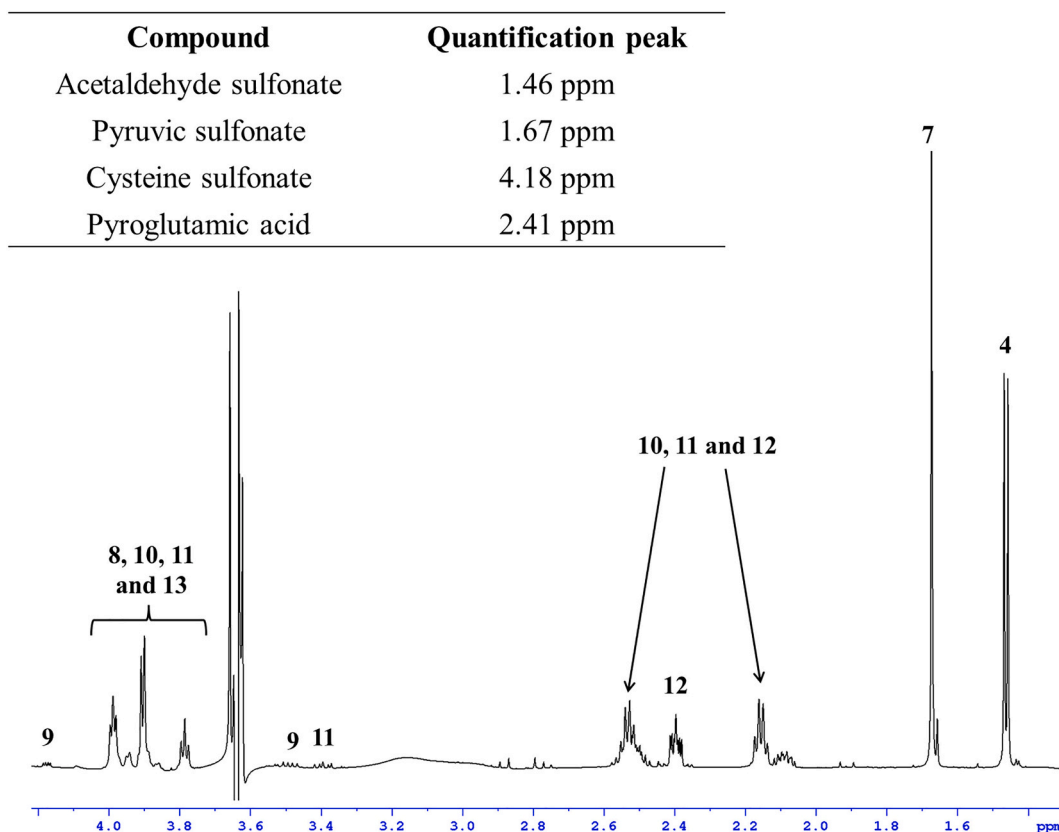


Fig. 2. ^1H NMR spectrum of free and SO_2 bound forms of **1**, **5**, **8** and **10** in mixture. Cysteinylglycine sulfonate was quantified indirectly by the peak of pyroglutamic acid. Acetaldehyde sulfonate (**4**), pyruvic sulfonate (**7**), cysteine (**8**), cysteine sulfonate (**9**), glutathione (**10**), glutathione sulfonate (**11**), pyroglutamic acid (**12**), cysteinylglycine sulfonate (**13**).

protons and their correlation with $\text{H1}'$, as well as a correlation between $\text{H5}'$ and the two $\text{H6}'$ that appear at 2.15 ppm and 2.54 ppm respectively, due to stereochemical reasons. HSQC (**Fig. S7**) showed the correlation between the protons of pyroglutamic acid, and their carbon and this assignment was consistent with the assignment given by databases and studies (<http://www.hmdb.ca/>, 2024; Koda et al., 2012). In the 2D HSQC experiment we also observed signals originating from proton-carbon pairs of the sulfonated dipeptide cysteinylglycine sulfonate (**13**). Their assignment was consistent with the respective assignment of glutathione sulfonate, with only small deviations in chemical shift. In the HMBC spectrum (**Fig. S8**), the correlation between proton $\text{H2}'$ and the carboxyl carbon (Cz) and proton $\text{H5}'$ and the carboxyl carbon (Cf) for glutathione is depicted. Moreover, the correlations between proton $\text{H1}'$ and the carbonyl carbon (Cy) as well as proton $\text{H3}'$ and the carboxyl carbon (Cx), were observed. It should also be noted that under our experimental conditions no trace of oxidized glutathione, GSSG, was detected in the NMR spectra of sulfonated GSH, and this was verified by comparison with reported literature data for GSSG (data not provided) (Kontogianni et al., 2017; Sharma et al., 2013).

For the quantification of compounds of interest in the NMR spectra, peaks in spectral regions clear of overlap were selected. These peaks are as follows: 1.46 ppm for acetaldehyde sulfonate, 1.67 ppm for pyruvic sulfonate and 4.18 ppm for cysteine sulfonate. However, the peaks of glutathione sulfonate were overlapped by other peaks, therefore, it was only possible to calculate the concentration of cysteinylglycine sulfonate. Although its peaks were also overlapped, the peak of pyroglutamic acid at 2.41 ppm could be used for the quantification of cysteinylglycine sulfonate since the two compounds were produced in equimolar amounts by the scission of sulfonated glutathione.

The characterization of the reaction products of the mixture was further confirmed after LC-QToF-MS analysis. The chromatogram of the

reaction mixture containing glutathione and SO_2 exhibited peaks corresponding to a majority of two sulfonated adducts (adducts **11** and **13**), both having a precursor ion (glutathione) with molecular mass of $m/z = 306.0765$ ($[\text{M} - \text{H}]^-$). These sulfonate mono-adducts had retention times of 0.65 and 0.68 min, respectively. Additionally, the formation of pyroglutamic acid was also confirmed after the identification of a peak at 0.75 min presenting a molecular mass of $m/z = 128.0350$ ($[\text{M} - \text{H}]^-$).

3.2. Kinetics of SO_2 binding of carbonyls and thiols under simulated barrel and bottle aging conditions

Based on the assignment of free and bound forms of the reaction mixture, the kinetic study of SO_2 binding was monitored under varying conditions of SO_2 and dissolved oxygen concentrations (**Fig. 3**). According to the literature, dissolved oxygen as well as total SO_2 levels decrease during bottle aging in a 2/1 ratio (SO_2/O_2) (Danilewicz & Standing, 2018; Ugliano, 2013). In this study, the binders/ SO_2 ratios 1/4 and 1/1 with dissolved oxygen at saturation, were used as experimental parameters to simulate barrel aging and bottle aging (at the very beginning) conditions, respectively. On the other hand, the binders/ SO_2 ratio 2/1 under anaerobic conditions (dissolved $\text{O}_2 < 1 \mu\text{g/L}$) was used to simulate late bottle aging conditions (> 2 years).

In our previous work, the impact of oxidation catalysts such as O_2 and iron II on the mechanism of sulfonation reaction of thiols has been addressed (Tachtalidou et al., 2024). This study clearly demonstrated that, under wine oxidation conditions, sulfonation products of thiols are formed. The derived sulfones are chemically stable (non-reversible), and their formation was promoted by the presence of iron and oxygen. Recent studies have also focused on how the formation and breakdown of polysulfanes from thiols are catalyzed by copper, with the involvement of SO_2 (Kreitman et al., 2017). However, in the current study, our

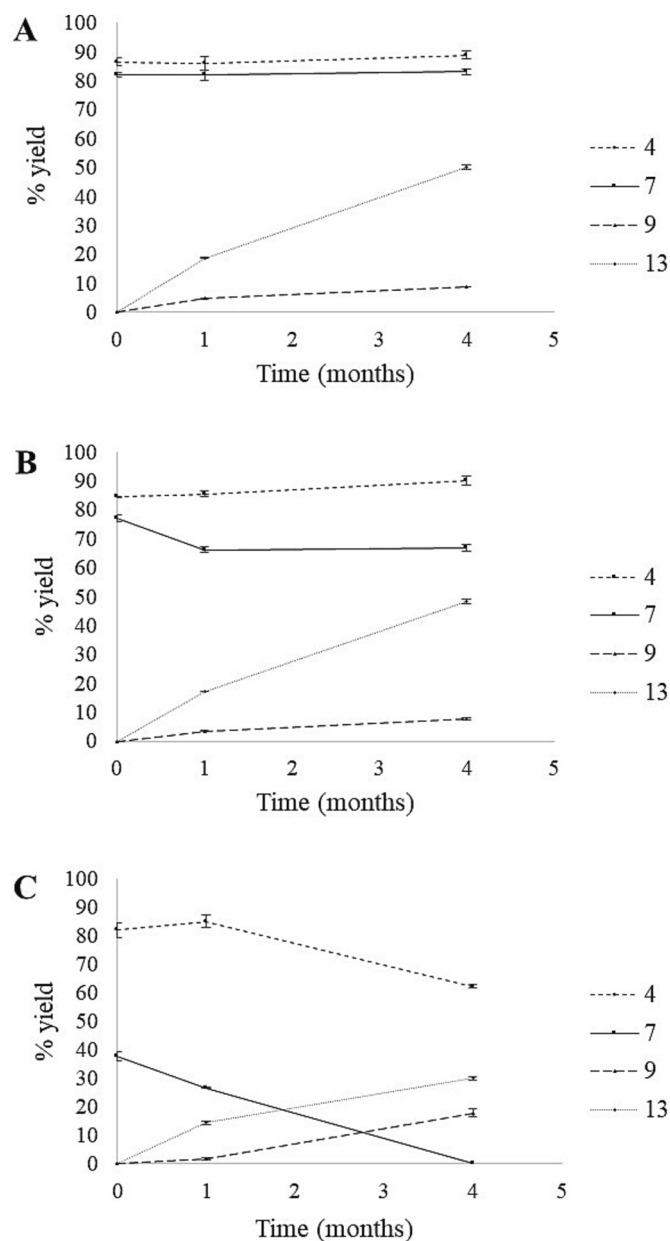


Fig. 3. Monitoring of sulfonation reactions in mixture in model wine (12% v/v ethanol, 5 g/L tartaric acid, pH 3.5) at room temperature in the context of, (A) barrel aging (binders / SO₂: 1/4; saturation of dissolved oxygen); (B) bottle aging at the very beginning (binders / SO₂: 1/1; anaerobic conditions) and (C) bottle aging at a later time (binders / SO₂: 2/1; anaerobic conditions). Acetaldehyde sulfonate (4), pyruvic sulfonate (7), cysteine sulfonate (9), cysteinylglycine sulfonate (13).

approach was to simplify the model solutions by examining the availability of oxygen and SO₂ without adding further reactions that occur simultaneously under real wine conditions.

The results presented in Fig. 3 show the potential of the binders to react with SO₂ in the presence of other compounds under different SO₂ and O₂ conditions. More specifically, it is shown that in all ratios, at t₀, only the formations of acetaldehyde and pyruvic sulfonate have occurred, an observation which is expected given that the equilibrium constants of these two compounds are 1.5×10^{-6} and 1.55×10^{-4} , respectively (Waterhouse et al., 2016). Although it was expected that the sulfonation reactions of acetaldehyde and pyruvic acid would be complete, the yields were between 40 and 85%. This could be explained by the interactions that occurred between binders. More specifically,

except of the reaction of acetaldehyde with glutathione, which is already known from the literature (Peterson & Waterhouse, 2016), acetaldehyde also reacts with cysteine forming 2-methylthiazolidine-4-carboxylic acid (Yamashita et al., 2010). Based on this, pyruvic acid could also possibly react with cysteine. Indeed, it has been already demonstrated that the concentration of pyruvic acid decreases in the presence of cysteine (Yoo et al., 2011) and it is well known that these two compounds react (Friedmann & Girsavicius, 1936), although the molecular formula of their reaction product has not been reported yet. In the present study, we observed and identified in the NMR spectra, minor products that could be due to the pyruvic acid/cysteine reaction, but their stereochemical configuration is still under investigation.

Continuing with the kinetics of the mixture after one month, the equilibrium has changed. Sulfonation of cysteine and glutathione has started under all experimental conditions. The yield of sulfonated adducts of acetaldehyde and pyruvic acid remain stable (error bars are significantly low) when SO₂ is in excess (Fig. 3A), while pyruvic sulfonate degraded when SO₂ was in a lower molecular ratio under both aerobic (Fig. 3B) and anaerobic (Fig. 3C) conditions. At month 4, the concentration of cysteine and glutathione sulfonated products increased in all modalities, while the dissociation of pyruvic sulfonate has started (Fig. 3B and C). Most interestingly, even if acetaldehyde sulfonate remains stable under aerobic conditions and high SO₂ concentration (Fig. 3A and B), it was observed that under anaerobic conditions (Fig. 3C) it degrades. This result indicates that there should be free SO₂ released from the carbonyls at month 4. In this experiment, the initial added ratio of binders/HSO₃⁻ was 2/1, meaning that insufficient amount of SO₂ was added for all available binders. Thus, if at t₀ the carbonyls (fast binding potential) have bound the majority of the available SO₂, at month 4, only the SO₂ released from the carbonyls should be available for binding. In that respect we conclude that at the late stages of bottle aging (Fig. 3C), SO₂ bound to carbonyls can be released and in turn bound to thiols, forming a strong and stable disulfide bond. These results are in accordance with previous published data indicating the possible dissociation of acetaldehyde sulfonate under wine oxidation conditions as well as the formation and stability of S-sulfonates under in absence of oxygen (Tachtalidou et al., 2022; Tachtalidou et al., 2024).

4. Conclusions

The sulfonation reactions of thiols and carbonyls were monitored under simulated barrel aging, bottle aging at the very beginning, and longer-term bottle aging conditions, by direct ¹H NMR spectroscopy. This study reports that during simulated wine aging, sulfur dioxide first bound to carbonyls is released and bind to cysteine and glutathione. This result demonstrates the long-term sulfur dioxide binding potential of S-containing compounds. This work supports the reconsideration of the categorization of SO₂ binders into strong and weak, since despite sulfur-containing compounds reacting slowly with sulfur dioxide, once they bind, the resulting disulfide bond is strong and the adducts remain stable over time.

CRediT authorship contribution statement

Sofia Tachtalidou: Writing – original draft, Data curation. **Apostolos Spyros:** Writing – original draft, Formal analysis, Data curation. **Nicolas Sok:** Data curation. **Silke S. Heinzmann:** Data curation. **Franck Denat:** Resources, Data curation. **Philippe Schmit-Kopplin:** Resources, Formal analysis, Data curation. **Régis D. Gougeon:** Writing – review & editing, Writing – original draft, Supervision, Project administration, Funding acquisition, Data curation, Conceptualization. **Maria Nikolantonaki:** Writing – review & editing, Writing – original draft, Visualization, Validation, Supervision, Resources, Investigation, Funding acquisition, Formal analysis, Data curation, Conceptualization.

Declaration of competing interest

The authors declare the following financial interests/personal relationships which may be considered as potential competing interests:

Maria Nikolantonaki reports financial support was provided by University of Burgundy Franche Comte. Maria Nikolantonaki reports a relationship with University of Burgundy Franche Comte that includes: funding grants.

Data availability

Data will be made available on request.

Acknowledgements

This work is part of the project MetaBox ISITE-BFC (2018-2021) supported by the Conseil Régional de Bourgogne Franche-Comté and the European Union through the PO FEDER-FSE Bourgogne 2014/2020 programs.

The authors also thank the Plateforme d'Analyse Chimique et de Synthèse Moléculaire de l'Université de Bourgogne (<http://www.wpcm.fr>) for access to NMR equipments and more specifically Michel Picquet, Quentin Bonnin and Marie-Jose Penouilh.

AS acknowledges support by the project "FoodOmicsGR_RI Comprehensive Characterization of Foods" (MIS 5029057) which is implemented under the Action "Reinforcement of the Research and Innovation Infrastructure", funded by the Operational Programme Competitiveness, Entrepreneurship and Innovation (NSRF 2014–2020) and co-financed by Greece and the European Union (European Regional Development Fund).

Appendix A. Supplementary data

Supplementary data to this article can be found online at <https://doi.org/10.1016/j.foodchem.2024.138944>.

References

- Aberl, A., & Coelho, M. (2013). Determination of sulfur dioxide in wine using headspace gas chromatography and electron capture detection. *Food Additives & Contaminants. Part A, Chemistry, Analysis, Control, Exposure & Risk Assessment*, *30*, 226–233.
- Arapitsas, P., Guella, G., & Mattivi, F. (2018). The impact of SO₂ on wine flavanols and indoles in relation to wine style and age. *Scientific Reports*, *8*, 858.
- Arapitsas, P., Speri, G., Angeli, A., Perenzoni, D., & Mattivi, F. (2014). The influence of storage on the "chemical age" of red wines. *Metabolomics*, *10*, 816–832.
- Bartowsky, E. J. (2009). Bacterial spoilage of wine and approaches to minimize it. *Letters in Applied Microbiology*, *48*, 149–156.
- Burroughs, L. F., & Sparks, A. H. (1973). Sulphite-binding power of wines and ciders. II. Theoretical consideration and calculation of sulphite-binding equilibria. *Journal of the Science of Food and Agriculture*, *24*, 199–206.
- Danilewicz, J. C., & Standing, M. J. (2018). Reaction mechanisms of oxygen and sulfite in red wine. *American Journal of Enology and Viticulture*, *69*, 17095.
- Deshmukh, M., Kutscher, H., Stein, S., & Sinko, P. (2009). Nonenzymatic, self-elimination degradation mechanism of glutathione. *Chemistry & Biodiversity*, *6*, 527–539.
- Friedman, M. (1996). Food Browning and its prevention: An overview. *Journal of Agricultural and Food Chemistry*, *44*, 631–653.
- Friedmann, E., & Girsavicius, J. (1936). Reactions of pyruvic acid with thiolacetic acid and cysteine. *Biochemical Journal*, *30*, 1886–1891.
- Goncalves, L. M., Grosso Pacheco, J., Jorge Magalhaes, P., Antonio Rodrigues, J., & Araujo Barros, A. (2010). Determination of free and total sulfites in wine using an automatic flow injection analysis system with voltammetric detection. *Food Additives & Contaminants. Part A, Chemistry, Analysis, Control, Exposure & Risk Assessment*, *27*, 175–180.
- <http://www.hmdb.ca/>, (2024).
- Karbowiak, T., Crouvisier-Urion, K., Lagorce, A., Ballester, J., Geoffroy, A., Roullier-Gall, C., ... Bellat, J.-P. (2019). Wine aging: A bottleneck story. *npj Science of Food*, *3*, 14.
- Koda, M., Furihata, K., Wei, F., Miyakawa, T., & Tanokura, M. (2012). NMR-based metabolic profiling of rice wines by F₂-selective total correlation spectra. *Journal of Agricultural and Food Chemistry*, *60*, 4818–4825.
- Kontogianni, V. G., Tsiafoulis, C. G., Roussis, I. G., & Gerotheranassis, I. P. (2017). Selective 1D TOCSY NMR method for the determination of glutathione in white wine. *Analytical Methods*, *9*, 4464–4470.
- Kreitman, G. Y., Danilewicz, J. C., Jeffery, D. W., & Elias, R. J. (2017). Copper(II)-mediated hydrogen sulfide and thiol oxidation to disulfides and organic polysulfanes and their reductive cleavage in wine: Mechanistic elucidation and potential applications. *Journal of Agricultural and Food Chemistry*, *65*, 2564–2571.
- Nikolantonaki, M., Julien, P., Coelho, C., Roullier-Gall, C., Ballester, J., Schmitt-Kopplin, P., & Gougeon, R. D. (2018). Impact of glutathione on wines oxidative stability: A combined sensory and metabolomic study. *Frontiers in Chemistry*, *6*, 182.
- Nikolantonaki, M., Magiatis, P., & Waterhouse, A. L. (2015). Direct analysis of free and sulfite-bound carbonyl compounds in wine by two-dimensional quantitative proton and carbon nuclear magnetic resonance spectroscopy. *Analytical Chemistry*, *87*, 10799–10806.
- Nikolantonaki, M., Romanet, R., Lucio, M., Schmitt-Kopplin, P., & Gougeon, R. (2022). Sulfonation reactions behind the fate of white wine's shelf-life. *Metabolites*, *12*(4).
- Peterson, A. L., & Waterhouse, A. L. (2016). 1H NMR: A novel approach to determining the thermodynamic properties of acetaldehyde condensation reactions with glycerol, (+)-catechin, and glutathione in model wine. *Journal of Agricultural and Food Chemistry*, *64*, 6869–6878.
- Romanet, R., Sarhane, Z., Bahut, F., Uhl, J., Schmitt-Kopplin, P., Nikolantonaki, M., & Gougeon, R. D. (2021). Exploring the chemical space of white wine antioxidant capacity: A combined DPPH, EPR and FT-ICR-MS study. *Food Chemistry*, *355*, Article 129566.
- Roullier-Gall, C., Hemmler, D., Gonsior, M., Li, Y., Nikolantonaki, M., Aron, A., ... Schmitt-Kopplin, P. (2017). Sulfites and the wine metabolome. *Food Chemistry*, *237*, 106–113.
- Roullier-Gall, C., Kanawati, B., Hemmler, D., Druschel, G. K., Gougeon, R. D., & Schmitt-Kopplin, P. (2019). Electrochemical triggering of the chardonnay wine metabolome. *Food Chemistry*, *286*, 64–70.
- Sharma, S. V., Arbach, M., Roberts, A. A., Macdonald, C. J., Groom, M., & Hamilton, C. J. (2013). Biophysical features of bacillithiol, the glutathione surrogate of *Bacillus subtilis* and other firmicutes. *Chembiochem*, *14*, 2160–2168.
- Stockley, C., Paschke-Kratz, A., Teissedre, P.-L., Restani, P., Garcia Tejedor, N., & Quini, C. (2021). *SO₂ and wines: A review* (1st ed.).
- Tachtalidou, S., Arapitsas, P., Penouilh, M.-J., Denat, F., Schmitt-Kopplin, P., Gougeon, R. D., & Nikolantonaki, M. (2024). Chemical stability of thiol and flavanol sulfonation products during wine aging conditions. *Journal of Agricultural and Food Chemistry*, *72*(4), 1885–1893.
- Tachtalidou, S., Sok, N., Denat, F., Noret, L., Schmitt-Kopplin, P., Nikolantonaki, M., & Gougeon, R. D. (2022). Direct NMR evidence for the dissociation of sulfur-dioxide-bound acetaldehyde under acidic conditions: Impact on wines oxidative stability. *Food Chemistry*, *373*, Article 131679.
- Ugliano, M. (2013). Oxygen contribution to wine aroma evolution during bottle aging. *Journal of Agricultural and Food Chemistry*, *61*, 6125–6136.
- Waterhouse, A., Sacks, G., & Jeffery, D. (2016). *Understanding wine chemistry*. John Wiley & Sons.
- Wissemann, K. W., & Lee, C. Y. (1980). Polyphenoloxidase activity during grape maturation and wine production. *American Journal of Enology and Viticulture*, *31*, 206–211.
- Yamashita, K., Noguchi, M., Mizukoshi, A., & Yanagisawa, Y. (2010). Acetaldehyde removal from indoor air through chemical absorption using L-cysteine. *International Journal of Environmental Research and Public Health*, *7*, 3489–3498.
- Yoo, K. S., Lee, E. J., & Patil, B. S. (2011). Underestimation of pyruvic acid concentrations by fructose and cysteine in 2,4-dinitrophenylhydrazine-mediated onion pungency test. *Journal of Food Science*, *76*, C1136–C1142.
- Zecchini, M., Lucas, R., & Le Gresley, A. (2019). New insights into the cysteine-sulfite reaction. *Molecules*, *24*.